Physics of Nuclei: Key Role of an Emergent Symmetry

T. Dytrych,[1,2] K. D. Launey,[1] J. P. Draayer,[1] D. J. Rowe,[3] J. L. Wood,[4] G. Rosensteel,[5] C. Bahri,[4] D. Langr,[6] and R. B. Baker[1]

[1]*Department of Physics and Astronomy, Louisiana State University, Baton Rouge, Louisiana 70803, USA*
[2]*Nuclear Physics Institute, Academy of Sciences of the Czech Republic, 250 68 Řež, Czech Republic*
[3]*Department of Physics, University of Toronto, Toronto, Ontario M5S 1A7, Canada*
[4]*School of Physics, Georgia Institute of Technology, Atlanta, Georgia 30332, USA*
[5]*Physics Department, Tulane University, New Orleans, Louisiana 70118, USA*
[6]*Faculty of Information Technology, Czech Technical University in Prague, 16000 Praha, Czech Republic*

(Received 18 July 2019; revised manuscript received 24 October 2019; published 28 January 2020)

We show through first-principles nuclear structure calculations that the special nature of the strong nuclear force determines highly regular patterns heretofore unrecognized in nuclei that can be tied to an emergent approximate symmetry. This symmetry is ubiquitous and mathematically tracks with a symplectic symmetry group. This, in turn, has important implications for understanding the physics of nuclei: we find that nuclei are made of only a few equilibrium shapes, deformed or not, with associated vibrations and rotations. It also opens the path for *ab initio* large-scale modeling of open-shell intermediate-mass nuclei without the need for renormalized interactions and effective charges.

DOI: 10.1103/PhysRevLett.124.042501

Introduction.—Exact symmetry and symmetry-breaking phenomena play a key role in providing a better understanding of the physics of many-particle systems, from quarks and nuclei, to molecules and galaxies. In atomic nuclei, exact and dominant symmetries such as rotational invariance, parity, and charge independence have been established. However, even when these symmetries are taken into account, the structure of nuclei remains illusive and only partially understood, with no additional symmetries immediately evident from the underlying interaction between protons and neutrons.

The nuclear shell model is based on the premise that nuclei have an underlying spherical harmonic oscillator (HO) shell structure [1], with residual interactions. In fact, with effective interactions (renormalized in the nuclear medium to a valence shell) and large effective charges that are introduced to account for missing collectivity, the shell model is successful at explaining many properties of nuclei. However, it has been much less successful at predicting the many surprises that surface, such as the highly collective rotational states that are described phenomenologically by the Bohr-Mottelson collective model [2], as well as the recognition that the first excited state of the doubly closed shell nucleus of ^{16}O is the head of a strongly deformed rotational band [3,4]. The coexistence of states of widely differing deformation in many nuclei is now well established [5–8] as an emergent phenomenon and dramatically exposes the limitations of the standard shell model.

To address this and to understand the physics of nuclei without limitations within the interaction and approximations during the many-body nuclear simulations, we use an *ab initio* framework that starts with realistic interactions tied to elementary particle physics considerations and fitted to nucleon-nucleon data. Such calculations are now possible and are able to give converged results for successful applications to structure and reactions of light nuclei by the use of supercomputers [9–21] with recent advances into the medium-mass region [22–25]. However, in *ab initio* calculations the complexity of the nuclear problem dramatically increases with the number of particles, and when expressed in terms of billions of shell-model basis states, the structure of a nuclear state is unrecognizable. But expressing it in a more informative basis, the symmetry-adapted (SA) collective basis [14,26], leads to a major breakthrough: in this Letter, we report on the remarkable outcome from first-principles investigations up through the intermediate-mass region, namely, the simplicity of nuclear low-lying states and the striking dominance of an associated symmetry of nuclear dynamics. Specifically, this is the symplectic $\mathrm{Sp}(3,\mathbb{R})$ symmetry, which together with its slight symmetry breaking is shown here to naturally emerge in atomic nuclei. This exposes for the first time the fundamental role of the $\mathrm{Sp}(3,\mathbb{R})$ symmetry and establishes it as a remarkably good symmetry of the strong nuclear force in the low-energy regime.

This emergent symplectic symmetry provides important new information through its link to nuclear collectivity: we show here that nuclei are made of only a few equilibrium shapes with associated vibrations and rotations. This pioneers *ab initio* descriptions that capitalize on the symplectic symmetry of open-shell intermediate-mass nuclei without the use of effective charges, with anticipated

predictions, e.g., for short-lived isotopes with large deformation or cluster substructure along various nucleosynthesis pathways, especially where experimental measurements are incomplete or not available.

It is known that SU(3), a subgroup of $\mathrm{Sp}(3,\mathbb{R})$, is the symmetry group of the spherical harmonic oscillator that underpins the shell model [1] and the valence-shell SU(3) Elliott model [27], which naturally describes rotations of a deformed nucleus without the need for breaking rotational symmetry. The key role of deformation in nuclei, along with the coexistence of low-lying states in a single nucleus with different quadrupole moments [5], makes the quadrupole moment $\langle Q \rangle$ a dominant fundamental property of the nucleus. Together with the monopole moment $\langle r^2 \rangle$ or "size" of the nucleus, it establishes the energy scale of the nuclear problem. Indeed, the nucleus size and shape underpin the essence of symplectic $\mathrm{Sp}(3,\mathbb{R})$ symmetry (see also Fig. 1 and Supplemental Material [28]). Not surprisingly, $\mathrm{Sp}(3,\mathbb{R})$, the underlying symmetry of the symplectic rotor model [29,30], has been found to play a key role across the nuclear chart—from the lightest systems [4,31], through intermediate-mass nuclei [14,32,33], up to strongly deformed nuclei of the rare-earth and actinide regions [30,34–36]. The results agree with experimental evidence that supports enhanced deformation and clustering in nuclei, as suggested by energy spectra, electric monopole and quadrupole transitions, radii, and quadrupole moments [5,37,38]. While these earlier models have successfully explained the observed collective patterns, they have assumed symmetry-based approximations. Only now, the present outcomes not only explain but also predict the emergence of nuclear collectivity across nuclei, even in close-to-spherical nuclear states without any recognizable rotational properties, as revealed within an *ab initio* framework without *a priori* symmetry assumptions, the symmetry-adapted no-core shell model (SA-NCSM) [14,26,39] with chiral effective field theory interactions.

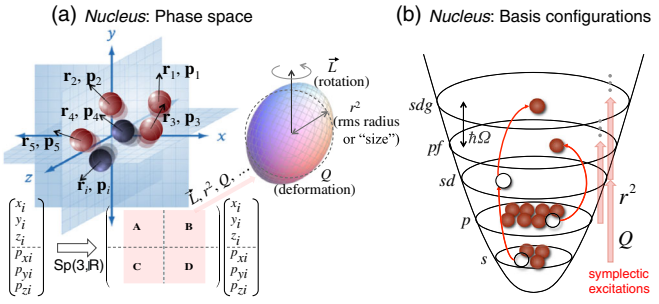

FIG. 1. (a) The symplectic group $\mathrm{Sp}(3,\mathbb{R})$ consists of all *particle-independent* linear canonical transformations $\left(\begin{smallmatrix} A & B \\ C & D \end{smallmatrix}\right)$ of the single-particle phase-space observables $\vec{r}_i$ (position) and $\vec{p}_i$ (momentum) that preserve the Heisenberg commutation relations $[r_{\alpha i}, p_{\alpha' j}] = i\hbar\delta_{\alpha\alpha'}\delta_{ij}$, $\alpha, \alpha' = x, y, z$ [40]. (b) In the shell model, the basis configurations are multiples of symplectic excitations, generated by r^2 and Q. A key feature is that a single-particle $\mathrm{Sp}(3,\mathbb{R})$ irreducible representation spans all positive-(or negative-)parity states for a particle in a 3D spherical or deformed harmonic oscillator.

SA-NCSM with $\mathrm{Sp}(3,\mathbb{R})$*-adapted basis.*—The SA-NCSM is based on the shell-model theory [9,41] that solves the many-body Schrödinger equation for A particles and, in its most general form, is an exact many-body "configuration interaction" method. The intrinsic nonrelativistic nuclear Hamiltonian includes the relative kinetic energy, nucleon-nucleon (NN) and, possibly, three-nucleon (3N) interactions, typically derived in the chiral effective field theory [42–45], along with the Coulomb interaction between the protons. We have adopted various realistic interactions without renormalization in nuclear medium, with results illustrated here for the Entem-Machleidt (EM) $\mathrm{N^3LO}$ [44] and $\mathrm{NNLO_{opt}}$ [46] chiral potentials. We neglect explicit 3N interactions, since they are known to be hierarchically smaller than NN.

New developments here focus on constructing the $\mathrm{Sp}(3,\mathbb{R})$-adapted basis (for computer codes, see Ref. [47]). This basis is built from the SU(3)-adapted basis reviewed in Ref. [14]. Briefly, each SU(3)-adapted basis state has definite proton (neutron) $S_{p(n)}$ and total S intrinsic spins, along with deformation-related $(\lambda\mu)\mathrm{SU}(3)$ quantum numbers and total number of HO quanta $N \leq N_{\max}$ ($N_{\max}$ is the same as the cutoff used in the conventional NCSM). The difficulty in constructing the symplectic basis stems from the fact that there are no known $\mathrm{Sp}(3,\mathbb{R})$ coupling or recoupling coefficients, and one has to resort to innovative techniques. Here, we adopt the SU(3) scalar operator $\{B^\dagger \times B\}^{(00)}_{L=0M=0}$, where the $\mathrm{Sp}(3,\mathbb{R})$ generator $B^\dagger$ moves a particle two shells up [arrows in Fig. 1(b)]. This operator is computed for a set of basis states with the same $N(\lambda\mu)S_pS_nS$; eigenvectors of this matrix realize $\mathrm{Sp}(3,\mathbb{R})$-adapted basis states and are used to construct the Hamiltonian in the new symplectic basis; the known eigenvalues are used to assign each eigenvector to a specific symplectic irreducible representation (irrep). While this procedure is computationally intensive, especially for higher-N sets of large dimensionality, the resulting Hamiltonian matrix is drastically small in size and its eigensolutions, the nuclear energies and states, can be calculated without the need for supercomputers.

Emergent symmetry and dominant nuclear features from first principles.—We report on the remarkable outcome, as unveiled from first-principles calculations below the calcium region, that nuclei exhibit relatively simple physics. We now understand that a low-lying nuclear state is predominantly composed of a few equilibrium shapes that vibrate and rotate, with each shape characterized by a single symplectic irrep.

To illustrate this, we consider the physics of ^{20}Ne (Fig. 2) and the contribution of a single symplectic irrep to its low-lying states, Fig. 2(a). Indeed, a single symplectic irrep can provide insight into the nuclear dynamics: as shown earlier [29,30,36,48] and discussed in the next paragraph, all

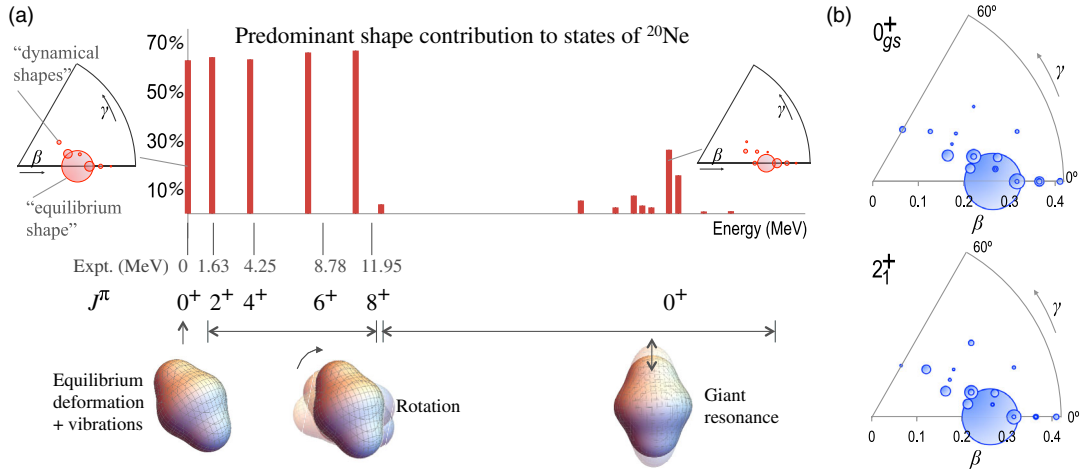

FIG. 2. (a) Excitation energies (horizontal axis) of the ground-state (gs) rotational band ($J^\pi = 0^+_{gs}, 2^+, 4^+, 6^+$, and 8^+) and excited 0^+ states in ^{20}Ne, shown together with the contribution to each state (vertical axis) of the single shape that dominates the ground state. According to this, states are grouped and schematically illustrated by "classical" shapes, vibrations, and rotations, where the *ab initio* one-body density profile in the *body-fixed* frame is shown for 0^+. (b) Deformation distribution of the equilibrium shapes that make up a state with contributions given by the area of the circles, specified by the average deformation β and triaxiality angle γ. Results are for *ab initio* SA-NCSM calculations with $\mathrm{NNLO_{opt}}$ for an SU(3) basis that yields a fast convergence of the gs rms radius (model space of 11 HO shells with $\hbar\Omega = 15$ MeV intershell distance).

configurations within a symplectic irrep preserve an equilibrium shape (or simply "shape") and realize its rotations, vibrations, and spatial orientations, implying that the ^{20}Ne *ab initio* wave functions for $J^\pi = 0^+_{gs}, 2^+, \ldots, 8^+$ shown in Fig. 2(a) indeed exhibit a predominance of a single shape that vibrates and rotates [see also, Fig. 2(b), largest circle].

To understand the relation of the symplectic symmetry to the shapes dynamics, we note that the quadrupole moment Q does not mix irreps. Hence, an average quadrupole ellipsoid can be assigned to each symplectic irrep. This is best understood in the limit of a valence shell, where the symplectic basis recovers the SU(3)-adapted basis of the Elliott model: a given many-particle SU(3) state can be associated with an average shape using the familiar shape parameters, deformation β and triaxiality γ, through the expectation values $\langle Q \cdot Q \rangle \sim \beta^2$ and $\langle [Q \times Q]_2 \cdot Q \rangle \sim \beta^3 \cos 3\gamma$ [49,50] [note that β and γ, while providing a physical meaning to $(\lambda\mu)$, describe average ellipsoids that lack details, e.g., as evident in the one-body densities of Fig. 2]. And since L is a good quantum number of each SU(3) state, it naturally informs about the rotations of this ellipsoid. Finally, the associated vibrations are described by the symplectic (particle-hole) excitations, here referred to as "dynamical shapes". This can be illustrated for a single spherical shape, where the symplectic excitations realize the microscopic counterpart of the surface vibrations of the Bohr-Mottelson collective model [48,51]. As further shown in the $\beta - \gamma$ plots of Fig. 2(a), the set of excited 0^+ states with nonnegligible contribution of the $1p$-$1h$ vibrations of the ground-state shape describes a fragmented giant monopole resonance (breathing mode) with a centroid around 29 MeV and a typical deformation content spread out to large β values due to vibrations [52].

The $\mathrm{Sp}(3,\mathbb{R})$-adapted basis is constructed for various nuclei, pointing to unexpectedly ubiquitous symplectic symmetry, with the illustrative examples for the odd-odd ^{6}Li, ^{8}He (considered to be spherical with a halo structure), and the intermediate-mass ^{20}Ne (Fig. 3). The outcome provides further evidence that nuclei are predominantly comprised (typically in excess of 70%–80%) of only a few shapes, often a single shape (a single symplectic irrep) as for ^{6}Li, ^{8}B, ^{8}Be, ^{16}O, and ^{20}Ne, or two shapes, e.g., for ^{8}He and ^{12}C [see Ref. [14] for ^{8}B and ^{8}Be based on SU(3) analysis, and [26] for ^{12}C and ^{16}O]. Hence, the ground state of ^{6}Li and ^{20}Ne (^{16}O) is found to exhibit a prolate (spherical) shape, while an oblate shape dominates in the case of ^{8}He. The same features, perhaps even more pronounced, are anticipated across the region of heavy nuclei where the symplectic symmetry has been originally adopted to explain deformation-related nuclear properties [30,34–36].

Besides the predominant irrep(s), there is a manageable number of symplectic irreps, each of which contributes at a level that is typically at least an order of magnitude smaller, as shown in Figs. 3(a)–3(c). Furthermore, the outcome implies that the richness of the low-lying excitation spectra naturally emerges from these shapes through their rotations, corroborating earlier results [53–55]. Indeed, practically the same symplectic content observed for the low-lying states in ^{6}Li, Fig. 3(a), and for those in ^{20}Ne, Fig. 3(c), is a rigorous signature of rotations of a shape and can be used to identify members of a rotational band. A notable outcome is that excitation energies and transition rates for a few symplectic

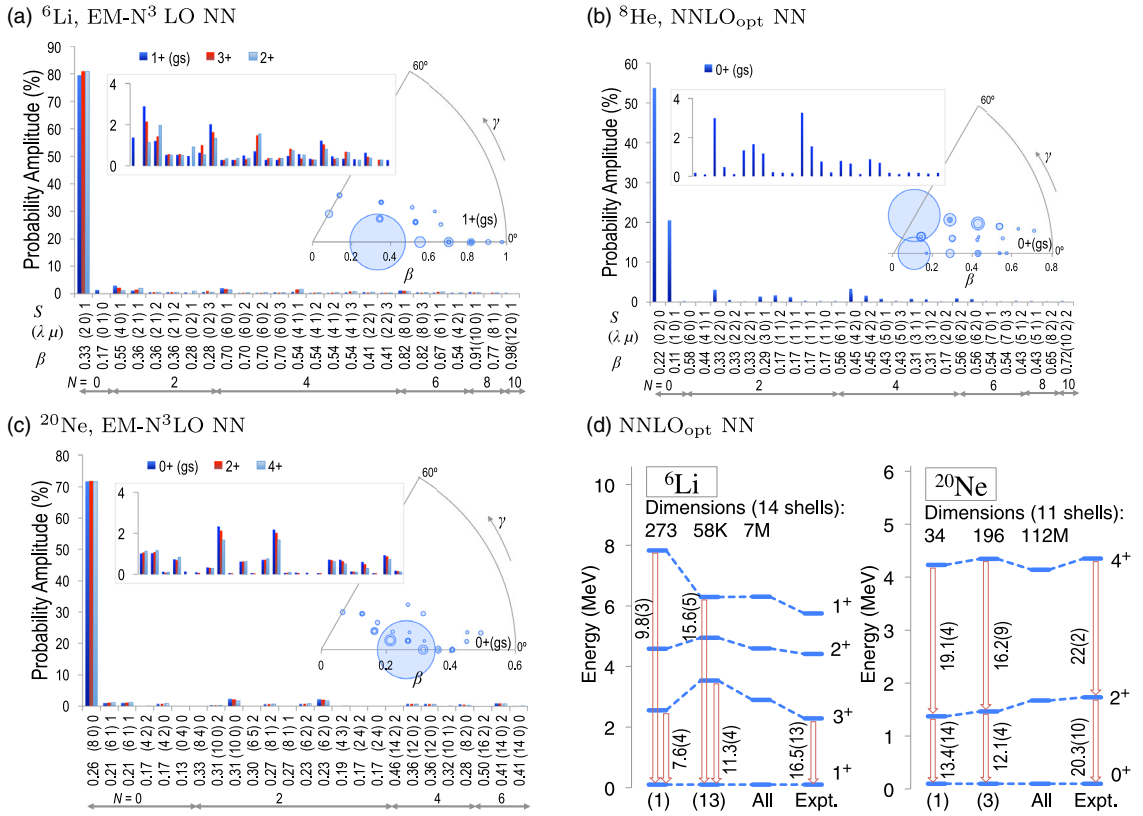

FIG. 3. (a)–(c) Symplectic $\mathrm{Sp}(3,\mathbb{R})$ irreps that make up the rotational band states of ^{6}Li, ^{8}He, and ^{20}Ne (in a close agreement with the results of Fig. 2); each irrep is specified by its equilibrium shape, labeled by β and the corresponding SU(3) labels $(\lambda\mu)$ together with total spin S. Insets: the same irreps but without the predominant contribution, together with the β-γ plot for the ground state. (d) Observables for ^{6}Li and ^{20}Ne calculated in the *ab initio* SA-NCSM with $\mathrm{Sp}(3,\mathbb{R})$ basis using only a small number (specified in the x-axis labels) dominant symplectic irreps including the most dominant one, as compared to experiment ("Expt."). Energies (with errors $\sim$100 keV) and $B(E2)$ transition strengths (in W.u.) are reported for extrapolations to infinitely many shells of converging results across variations in the model space size and resolution (see Supplemental Material [28]). Model-space dimensions are shown above each case; for comparison, the corresponding NCSM dimension for $J^\pi = 0^+, 2^+, 4^+$ in ^{20}Ne in 11 HO shells is 3.8×10^{10}. Results (a)–(c) and energies in (d) labeled as "All" are reported for *ab initio* SA-NCSM calculations for an SU(3) basis that yields a fast convergence of the gs rms radius: complete (selected) model space of 14 (11) HO major shells for ^{6}Li and ^{8}He (^{20}Ne) with intershell distance of (a)–(b) 20 and (c)–(d) 15 MeV.

irreps closely reproduce the experimental data, Fig. 3(d), and remain stable as the number of symplectic irreps is varied. Extrapolations to the infinite number of shells use the Shanks transformation and are based on the fast convergence we find for observables [56,57].

Radii and $E2$ transitions are determined by $\mathrm{Sp}(3,\mathbb{R})$ generators (r^2 and Q, respectively) that do not mix symplectic irreps. The predominance of a single symplectic irrep reveals the remarkable result that the largest fraction of these observables, and hence nuclear size and collectivity, necessarily emerges within this symplectic irrep, Fig. 3(d). We note that the underprediction of the $E2$ transitions agrees with rms radii estimates, as both observables exhibit almost perfect correlations (see Supplemental Material [28]). This also implies that the inclusion of 3N forces, currently work in progress, will have an effect on the $E2$ estimates, albeit to a small degree: e.g., rms radii decrease by about 3% for light nuclei with EM-N^{3}LO NN + 3N [58]; further, the extrapolated rms matter radii for NNLO$_{opt}$ NN deviate from experiment only by 2% for ^{6}Li and 6.7% for ^{20}Ne (see also Ref. [20]). Indeed, as shown in Figs. 2 and 3, the symmetry patterns for the EM-N^{3}LO, whose complementary 3N forces give non-negligible contributions to binding energies and radii, exhibit a strikingly similar behavior to the ones for NNLO$_{opt}$ that minimizes such 3N contribution in ^{3}H and ^{3,4}He [46].

The outcome is not sensitive to the parameters of the basis, $\hbar\Omega$ and $N_{\max}$. These model parameters can be related to L_{eff}, the infrared IR cutoff, and a_{eff}, the ultraviolet UV cutoff $\Lambda_{\mathrm{eff}} = 1/a_{\mathrm{eff}}$ [59], which can be understood as the effective size of the model space ("box") in which the nucleus resides and its grid size (resolution), respectively. Indeed, the symplectic content of a nucleus is found to be stable against variations in the box size or resolution (Fig. 4). This has an important implication: complete SA-NCSM calculations are

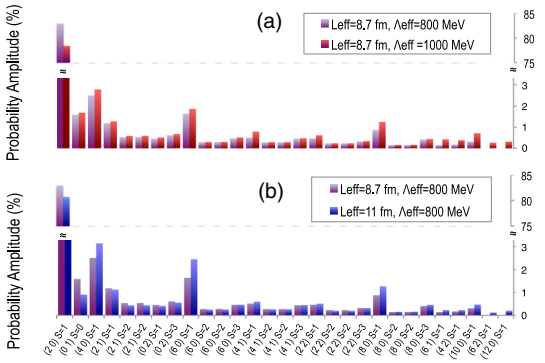

FIG. 4. Symplectic $\mathrm{Sp}(3,\mathbb{R})$ irreps, labeled by $(\lambda\mu)S$, that make up the ground state of ^{6}Li, as calculated by the *ab initio* SA-NCSM with SU(3) basis with the N^{3}LO interaction and the effect on the symplectic content (a) as the resolution improves (grid size decreases) for the same box size, and (b) as the box size increases for the same resolution. No new dominant equilibrium shapes are observed as the box size or grid resolution increases.

performed in smaller box sizes and/or low resolution to identify the nonnegligible symplectic irreps, while the model space is then augmented by extending these irreps to high (otherwise inaccessible) HO major shells to accommodate collective and spatially enhanced modes.

In short, this work shows that nuclei up through the intermediate-mass region and their low-energy excitations display relatively simple emergent physics that is collective in nature and tracks with an approximate symplectic symmetry heretofore gone unrecognized in the strong nuclear force. This work may have potential impacts, in general, to studies of strongly interacting quantum systems, e.g., incorporating emergent symmetries into tensor network quantum states.

We acknowledge helpful discussions with James P. Vary, Pieter Maris, and Calvin Johnson. This work was supported by the U.S. National Science Foundation (OIA-1738287, ACI -1713690, PHY-1913728), the Czech Science Foundation (16-16772S), the Czech Ministry of Education, Youth and Sports under (CZ.02.1.01/0.0/0.0/16_019/0000765), and SURA. This work benefited from computing resources provided by Blue Waters (supported by the National Science Foundation Grants No. OCI-0725070 and No. ACI-1238993, and the state of Illinois), Louisiana State University, and the National Energy Research Scientific Computing Center NERSC (a DOE Office of Science User Facility supported by the Office of Science of the U.S. Department of Energy under Contract No. DE-AC02-05CH11231).

[1] M. G. Mayer and J. H. D. Jensen, *Elementary Theory of Nuclear Shell Structure* (Wiley, New York, 1955).
[2] A. Bohr and B. R. Mottelson, Mat. Fys. Medd. K. Dan. Vidensk. Selsk **27**, No. 16 (1953).
[3] H. Morinaga, Phys. Rev. **101**, 254 (1956).
[4] D. J. Rowe, G. Thiamova, and J. L. Wood, Phys. Rev. Lett. **97**, 202501 (2006).
[5] K. Heyde and J. L. Wood, Rev. Mod. Phys. **83**, 1467 (2011).
[6] D. J. Rowe and J. L. Wood, *Fundamentals of Nuclear Models: Foundational Models* (World Scientific, Singapore, 2010).
[7] J. L. Wood, in *Emergent Phenomena in Atomic Nuclei from Large-Scale Modeling: A Symmetry-Guided Perspective*, edited by K. D. Launey (World Scientific Publishing Co., Singapore, 2017), ISBN 978-981-3146-04-4.
[8] P. E. Garrett *et al.*, Phys. Rev. Lett. **123**, 142502 (2019).
[9] B. Barrett, P. Navrátil, and J. Vary, Prog. Part. Nucl. Phys. **69**, 131 (2013).
[10] G. Hagen, T. Papenbrock, D. J. Dean, and M. Hjorth-Jensen, Phys. Rev. Lett. **101**, 092502 (2008).
[11] E. Epelbaum, H. Krebs, D. Lee, and Ulf-G. Meißner, Phys. Rev. Lett. **106**, 192501 (2011).
[12] K. Tsukiyama, S. K. Bogner, and A. Schwenk, Phys. Rev. Lett. **106**, 222502 (2011).
[13] S. Bacca, N. Barnea, W. Leidemann, and G. Orlandini, Phys. Rev. Lett. **110**, 042503 (2013).
[14] K. D. Launey, T. Dytrych, and J. P. Draayer, Prog. Part. Nucl. Phys. **89**, 101 (2016).
[15] T. Abe, P. Maris, T. Otsuka, N. Shimizu, Y. Utsuno, and J. P. Vary, Phys. Rev. C **86**, 054301 (2012).
[16] A. Cipollone, C. Barbieri, and P. Navratil, Phys. Rev. Lett. **111**, 062501 (2013).
[17] S. Elhatisari, D. Lee, G. Rupak, E. Epelbaum, H. Krebs, T. A. Lähde, T. Luu, and U.-G. Meißner, Nature (London) **528**, 111 (2015).
[18] E. Gebrerufael, K. Vobig, H. Hergert, and R. Roth, Phys. Rev. Lett. **118**, 152503 (2017).
[19] S. Pastore, A. Baroni, J. Carlson, S. Gandolfi, S. C. Pieper, R. Schiavilla, and R. B. Wiringa, Phys. Rev. C **97**, 022501(R) (2018).
[20] M. Burrows, C. Elster, S. P. Weppner, K. D. Launey, P. Maris, A. Nogga, and G. Popa, Phys. Rev. C **99**, 044603 (2019).
[21] G. Hupin, S. Quaglioni, and P. Navrátil, Nat. Commun. **10**, 351 (2019).
[22] T. Duguet, V. Somà, S. Lecluse, C. Barbieri, and P. Navrátil, Phys. Rev. C **95**, 034319 (2017).
[23] K. D. Launey, A. Mercenne, G. H. Sargsyan, H. Shows, R. B. Baker, M. E. Miora, T. Dytrych, and J. P. Draayer, AIP Conf. Proc. **2038**, 020004 (2018).
[24] T. D. Morris, J. Simonis, S. R. Stroberg, C. Stumpf, G. Hagen, J. D. Holt, G. R. Jansen, T. Papenbrock, R. Roth, and A. Schwenk, Phys. Rev. Lett. **120**, 152503 (2018).
[25] P. Gysbers *et al.*, Nat. Phys. **15**, 428 (2019).
[26] T. Dytrych, K. D. Sviratcheva, C. Bahri, J. P. Draayer, and J. P. Vary, Phys. Rev. Lett. **98**, 162503 (2007).
[27] J. P. Elliott, Proc. R. Soc. A **245**, 128 (1958).
[28] See Supplemental Material at http://link.aps.org/supplemental/10.1103/PhysRevLett.124.042501 for properties of the symplectic $\mathrm{Sp}(3,\mathbb{R})$ group, extrapolation calculations, and correlation plots.
[29] G. Rosensteel and D. J. Rowe, Phys. Rev. Lett. **38**, 10 (1977).
[30] D. J. Rowe, Rep. Prog. Phys. **48**, 1419 (1985).
[31] A. C. Dreyfuss, K. D. Launey, T. Dytrych, J. P. Draayer, and C. Bahri, Phys. Lett. B **727**, 511 (2013).

[32] J. P. Draayer, K. J. Weeks, and G. Rosensteel, Nucl. Phys. **A413**, 215 (1984).
[33] G. K. Tobin, M. C. Ferriss, K. D. Launey, T. Dytrych, J. P. Draayer, A. C. Dreyfuss, and C. Bahri, Phys. Rev. C **89**, 034312 (2014).
[34] O. Castaños, P. Hess, J. Draayer, and P. Rochford, Nucl. Phys. **A524**, 469 (1991).
[35] M. Jarrio, J. L. Wood, and D. J. Rowe, Nucl. Phys. **A528**, 409 (1991).
[36] C. Bahri and D. J. Rowe, Nucl. Phys. **A662**, 125 (2000).
[37] J. Henderson *et al.*, Phys. Lett. B **782**, 468 (2018).
[38] M. Freer, H. Horiuchi, Y. Kanada-En'yo, D. Lee, and Ulf-G. Meißner, Rev. Mod. Phys. **90**, 035004 (2018).
[39] T. Dytrych, K. D. Launey, J. P. Draayer, P. Maris, J. P. Vary, E. Saule, U. Catalyurek, M. Sosonkina, D. Langr, and M. A. Caprio, Phys. Rev. Lett. **111**, 252501 (2013).
[40] D. J. Rowe, in *Emergent Phenomena in Atomic Nuclei from Large-Scale Modeling: A Symmetry-Guided Perspective*, edited by K. D. Launey (World Scientific Publishing Co., Singapore, 2017), ISBN 978-981-3146-04-4.
[41] E. Caurier, G. Martinez-Pinedo, F. Nowacki, A. Poves, and A. P. Zuker, Rev. Mod. Phys. **77**, 427 (2005).
[42] P. F. Bedaque and U. van Kolck, Annu. Rev. Nucl. Part. Sci. **52**, 339 (2002).
[43] E. Epelbaum, A. Nogga, W. Glöckle, H. Kamada, Ulf-G. Meißner, and H. Witala, Phys. Rev. C **66**, 064001 (2002).
[44] D. R. Entem and R. Machleidt, Phys. Rev. C **68**, 041001(R) (2003).
[45] E. Epelbaum, Prog. Part. Nucl. Phys. **57**, 654 (2006).
[46] A. Ekström, G. Baardsen, C. Forssén, G. Hagen, M. Hjorth-Jensen, G. R. Jansen, R. Machleidt, W. Nazarewicz *et al.*, Phys. Rev. Lett. **110**, 192502 (2013).
[47] T. Dytrych, LSU3shell code, Louisiana State University, available under the GNU General Public License at the *git* repository, http://sourceforge.net/projects/lsu3shell (2013).
[48] D. J. Rowe, arXiv:1909.07188.
[49] O. Castaños, J. P. Draayer, and Y. Leschber, Z. Phys. A **329**, 33 (1988).
[50] M. T. Mustonen, C. N. Gilbreth, Y. Alhassid, and G. F. Bertsch, Phys. Rev. C **98**, 034317 (2018).
[51] D. Rowe, AIP Conf. Proc. **1541**, 104 (2013).
[52] C. Bahri, J. P. Draayer, O. Castaños, and G. Rosensteel, Phys. Lett. B **234**, 430 (1990).
[53] T. Dytrych, K. D. Sviratcheva, C. Bahri, J. P. Draayer, and J. P. Vary, Phys. Rev. C **76**, 014315 (2007).
[54] P. Maris, M. A. Caprio, and J. P. Vary, Phys. Rev. C **91**, 014310 (2015).
[55] C. W. Johnson, Phys. Rev. C **91**, 034313 (2015).
[56] D. Shanks, J. Math. Phys. (N.Y.) **34**, 1 (1955).
[57] C. Bender and S. Orszag, *Advanced Mathematical Methods for Scientists and Engineers* (Springer, New York, 1999), ISBN 978-0-387-98931-0.
[58] P. Maris, J. P. Vary, and P. Navrátil, Phys. Rev. C **87**, 014327 (2013).
[59] K. A. Wendt, C. Forssén, T. Papenbrock, and D. Sääf, Phys. Rev. C **91**, 061301(R) (2015).